Auditory mechanics of the frog basilar papilla

Schoffelen, Richard Leonard Maria

CHAPTER 3

Detailed anatomy of the leopard frog's basilar papilla

R.L.M. Schoffelen
J.M. Segenhout
P. van Dijk

Abstract:
The basilar papilla is one of two dedicated auditory end organs in the frog inner ear. Due to the lack of a basilar membrane (BM), it appears to be a functionally and anatomically simpler organ than found in other vertebrates.
In this paper we present a detailed description of the basilar papilla (BP) of the northern leopard frog (*R. pipiens pipiens*) based on scanning-electron-microscopy (SEM) and light-microscopy (LM) images. Our findings are in line with those reported earlier in related species, and form a basis for the interpretation of the mechanical measurements on the basilar papilla.

3.1 Introduction

Anatomical studies provide a valuable addition to physiological and mechanical measurements for understanding the functioning of the inner ear. Besides forming the basis of modeling approaches, they provide hypotheses for the mechanics of the various structures in the inner ear.

Due to its relatively simple anatomy and physiology the frog inner ear provides us with a unique opportunity to study fundamental processes in vertebrate hearing. The frog inner ear contains eight sensory epithelia for the senses of hearing and balance (Wever 1985; Schoffelen et al. 2008, chapter 2), including two end organs dedicated to the detection of auditory signals: the amphibian papilla (AP) and the BP. While both the AP and the BP have sensory hair cells, neither has the BM that is present in all other terrestrial vertebrates as a flexible substrate for these cells. This, presumably, makes the inner-ear mechanics in the frog less complex than those in, for example, mammals. Both of the frog's auditory end organs have a tectorial membrane (TM) that covers the entire or part of the sensory epithelium.

The AP is the frog's low-frequency detector. Its anatomy exhibits considerable variations across species (Lewis 1984). The AP has a tonotopic organization with the detected frequencies increasing from the rostral to the caudal side of the organ (Lewis et al. 1982). The species-dependent upper limit is between 0.4 and 1.4 kHz, and is correlated with the length of the organ's extension in the caudal direction (Lewis 1981; Simmons et al. 2007). The BP covers the high-frequency part of the frog's auditory range. This organ is tuned to a single frequency that varies between species and individuals of the same species (Capranica and Moffat 1983). It may be as low as 1.0 to 1.5 kHz in the bullfrog (Shofner and Feng 1981; Ronken 1991), and as high as 2.5 to 3.9 kHz in *Hyla cinerea* (Ehret and Capranica 1980) or *Eleutherodactylus coqui* (Narins and Capranica 1980). In the leopard frog, it is approximately between 1.2 and 2.5 kHz (Ronken 1990; Ronken 1991; Smotherman and Narins 2000; Schoffelen et al. 2009b, chapter 4).

In anuran species, the BP is located in a tubular recess that extends directly from the saccular space (Van Bergeijk 1957; Frishkopf and Flock 1974; Lewis and Narins 1999). It ends at the contact membrane (CM), which forms the separation between the endolymphatic space within the recess and the perilymphatic space beyond it. The epithelium of the anuran BP lies deeply within the recess. This is in contrast with the BP in many other amphibians, where the BP may cover all of its recess and extend into the lagenar recess (caecilians and

urodeles, Lewis and Narins 1999).

The anuran BP's TM is a thin semicircular structure that extends from the hair cells closest to the contact membrane to a strand of tectorial material spanning the width of the papillar recess (fig. 3.3; Lewis and Narins 1999). This strand is also referred to as the 'terminal chord' (Van Bergeijk 1957; Bergeijk and Witschi 1957; Geisler et al. 1964). Along part of its semicircular edge, the TM connects to the hair cells of the epithelium. The two or three rows of hair cells closest to the contact membrane appear to extend into pores in the TM, while the other hair cells may not be directly connected to the TM (Lewis 1977; Lewis and Narins 1999).

In the various organs of the anuran inner ear, a variety of different inner-hair-cell types is found (Lewis and Li 1975; Smotherman and Narins 1999a). However, there are none similar to mammalian outer hair cells among them. Within the BP of the bullfrog, Lewis and Li (1975) identify three different types of hair cells based on the morphology of their stereovillar bundle. The stereovilli in all three types are organized in an systematic manner from shortest to tallest villi. The hair cell is maximally sensitive for deflection towards the longest villus, the kinocilium. This direction is defined as the hair-cell polarization. Mappings of the hair-cell polarizations within an epithelium give an indication of the presumed predominant direction of deflection of the hair bundles, and through it an insight into the mechanics of the inner ear. Hair-cell polarization maps of the BP show rather wide variations between anuran species. However, in species with the most derived inner ears, including *Rana, Xenopus* and *Pipa* the hair-cell polarization is uniformly from the sacullar side of the papilla to the CM (Lewis et al. 1985; Lewis and Narins 1999).

Recently, functional studies in the anurans from the *Rana*-family have been predominantly performed in either the bullfrog, *R. catesbeiana*, (e.g. Yu et al. 1991; Martin and Hudspeth 1999; Purgue and Narins 2000a; Bozovic and Hudspeth 2003) or the leopard frog, *R. pipiens* (e.g. Ronken 1990; Benedix et al. 1994; Van Dijk et al. 2002; Meenderink 2005). Anatomical studies of the basilar papilla in this family have been largely confined to the bullfrog (Geisler et al. 1964; Frishkopf and Flock 1974; Lewis 1977; Auer et al. 2008), although other species were studied as well (Wever 1985). In this paper, we report on a detailed exploration of the BP of the northern leopard frog, *Rana pipiens pipiens*. Our findings corresponded closely to those reported in the bullfrog (Frishkopf and Flock 1974) and other members of the *Rana*-family (Wever 1985).

3.2 Materials and methods

Inner-ear specimens were used from northern leopard frogs that were killed for the investigation of the mechanical response of the TM (Schoffelen et al. 2009b, chapter 4; Schoffelen et al. 2009a, chapter 5). The animal experiments were conducted in compliance with the current legislation in the Netherlands. Part of these requirements is the approval of the experimental procedure by the Institutional Animal Care and Use Committee prior to the start of the measurements.

The animals were obtained from a commercial supplier (Charles D. Sullivan Co. Inc., Nashville (TN), USA via Exoterra Schaudi GmbH, Holzheim, Germany). They were killed using a double-pith procedure, and the ears were excised. After excision, the ears were kept submerged in amphibian ringer solution (Carolina Biological Supply Company, Burlington (NC), USA), while the endolymphatic space remained closed. For SEM and LM imaging, we

used BP's from ears that were used for TM-response measurements (Schoffelen et al. 2009b, chapter 4; Schoffelen et al. 2009a, chapter 5), as well as from ears that were not included in those measurements.

Of the ears to be used for imaging, the otic capsules were opened and the BP lumina were isolated. The BPs were then fixated by immersion in a solution of 2.5% glutaraldehyde in 0.1-M Na-cacodylate buffer (pH = 7.4; 400 Mosm) and 2 mM calcium chloride. Some of the BPs were subsequently prepared for scanning electron microscopy (SEM), while others were used for light miscroscopy (LM).

Scanning Electron Microscopy Post-fixation for SEM imaging was performed according to the OTOTO non-coating technique (OsO_4 - Thiocarbohydrazide - OsO_4 - Thiocarbohydrazide - OsO_4; Malick and Wilson 1975). This technique involves alternating submersion of the preparation in OsO_4 (in a 0.1 M Na-cacodylate buffer) and in the ligand thiocarbohydrazide, as prescribed by the OTOTO sequence (detailed in Jongebloed et al. 1992). After post-fixation, the BP preparations were dehydrated in a graded ethanol series (30% vol.-50-70-90-100-100). Finally, they were critical-point dried with liquid carbon dioxide.

The resulting preparations were studied with a field-emission gun scanning microscope (type 6301F, JEOL Ltd, Tokyo, Japan), operated between 2 and 3 kV.

Light microscopy For LM, post-fixation was performed by submerging the BP in a solution of 1% OsO_4 and 1% $K_4Ru(CN)_6$ for two to three hours, followed by careful rinsing with distilled water. Subsequently, the specimen was dehydrated in a graded ethanol series, followed by submersion in propylene oxide. It was then infiltrated for two hours with a 1:1 mixture of propylene oxide and Spurr's low-viscosity resin, followed by over-night infiltration with pure Spurr's resin. Afterwards, resin polymerization took place at 70°C.

Semi-thin ($\sim$ 1 μm) sections were cut of the resin-encapsulated BPs, and stained with toluidine blue. The stained sections were analyzed under a light microscope (type DM-RXA, Leica Microsystems GmbH, Wetzlar, Germany).

Non-fixated preparations During fixation and post-fixation, any soft tissue in the preparation may be dislocated, distorted and reduced in volume, due to the dehydrating treatment. In the SEM and LM images, we observed significant reduction of the TM in the BP. Therefore, photos of non-fixated preparations were used to complement the observations from the SEM and LM images. The photos were taken as part of the mechanical-response measurements (Schoffelen et al. 2009b, chapter 4; Schoffelen et al. 2009a, chapter 5), using an optical micoscope (BX51WI, Olympus Corporation, Japan) equipped with a scientific-grade monochrome digital camera (1412TE Cooler Camera, DVC Company, Austin, TX, USA). For these measurements, the perilymphatic space had been opened at the round window. Images were taken through the BP's CM, while the endolymphatic space remained closed. Thus, the images show the BP in a fresh preparation in its normal fluid environment.

3.3 Results

The leopard frog's BP is situated in its own recess in the wall of the saccular space. The sensory epithelium is located on the dorsal wall of the lumen. An SEM overview of the

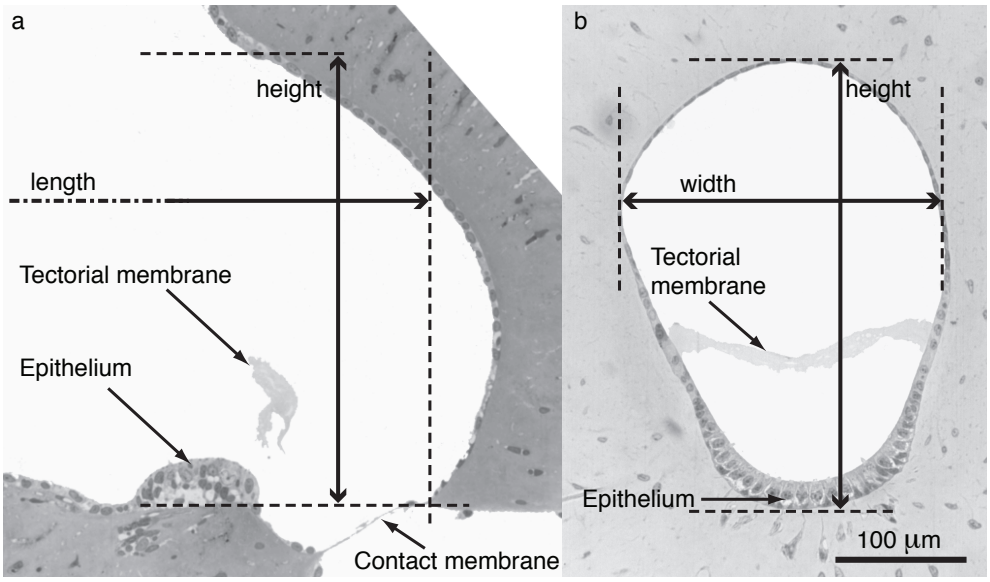

Figure 3.1: LM images of the BP. The left panel (a) was taken from a slice along the length of the epithlium, the right panel (b) perpendicular to it. Key structures in the BP are indicated, as well as the directions along which various dimensions of the lumen were determined. The TM is reduced in size and detached from the epithelium due to the preparation process.

basilar papilla in its lumen is displayed in figure 3.3[1]. The lumen is roughly cylindrical in shape. Its opening into the saccular space forms the lateral end of the lumen. The medial end is partially formed by the CM (fig. 3.1a).

3.3.1 The BP's lumen

For the purpose of this description we defined the length of the lumen to be parallel to the basal side of the epithelium (fig. 3.1a). This direction is parallel to the predominant hair-cell orientation (see below), and coincides with the measured direction of motion of the TM (Schoffelen et al. 2009a, chapter 5). A cross-section perpendicular to the length was approximately oval in shape over most of the length of the lumen (fig. 3.1b), while it was more circular between the epithelium and the CM. The short axis of the oval cross section is called the width of the lumen, while the long axis is the height.

The length of the lumen was estimated to be in the order of 500 μm. Its height decreased regularly from the lateral (saccular) to the medial (CM) side. Based on LM images, the taper was determined to be between 20° and 40° across preparations. Along the length of the sensory epithelium ($\sim$ 100 μm, fig. 3.1a) the average lumen height ranged from 350 μm to 400 μm across ears.

The width of the lumen varied in a less regular manner. It was constant at approximately 270 μm over the length of the epithelium. Between the epithelium and the saccular space, the

[1] As is customary in descriptions of the frog basilar papilla (e.g. Van Bergeijk 1957; Frishkopf and Flock 1974; Wever 1985; and Lewis and Narins 1999) we chose to display it with the epithelium at the bottom of the lumen throughout this paper.

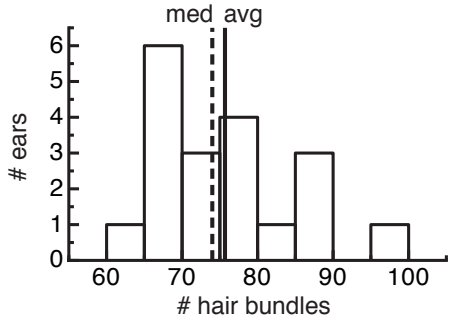

Figure 3.2: Histogram of hair-cell counts in 19 BPs. The number of hair-cells was determined by counting the hair bundles in SEM images. The dashed and the solid vertical line indicate the median (med) and the average (avg), respectively.

width decreased slightly before widening into the saccular space.

3.3.2 The epithelium

The epithelium of the BP was located approximately 50 μm from the CM at the medial end of its recess. Its total length was approximately 100 μm. The epithelium consisted of sensory hair cells, and supporting cells covered with microvilli.

The hair cells occupied an approximately rectangular area on the curved lumen boundary. This area measured about 55 μm (SEM, n=4, range 53-64 μm) along the length of the lumen, and 275 μm (LM, n=4, range 224-340 μm) along the curved perimeter of the lumen (width). Across the specimens examined in SEM, the number of hair cells ranged from 63 to 95 (average=76, median=74). In figure 3.2, a histogram is displayed of the hair-cell counts in 19 preparations.

The hair cells were set in six to eight rows. The two to three rows closest to the CM generally had a dense and a regular organization (fig. 3.4), while those closer to the saccular space appeared to be set in a more random pattern.

Based on the shape of the hair bundles, we identified four types of hair cells (SEM, fig. 3.5). In the first type (type D, classification according to Lewis and Li 1975), the hair bundles were circular with a relatively low maximum villus length ($\sim$ 3-4 μm), a small slope from the shortest to the longest villus ($\sim 35^\circ$), and a bulbed kinocilium. In the second type (type F), the maximum villus length was higher ($\sim$ 5-8 μm) and the slope steeper ($\sim 55^\circ$); the kinocilium was unbulbed. The third type (type E) was similar to the type-F cells, except this type had a bulbed kinocilium. The third type (type A) had relatively short stereovilli and a tall unbulbed kinocilium with a length in the same range as the maximum length in the type-F and type-E cells ($\sim$ 5-8 μm). On average, all four types of hair cells had approximately 30 stereovilli. The stereovilli in the type-A cells were thinner, resulting in a smaller diameter of the hair bundle than in the other three types.

Type-D cells occupied the larger part of the first two to three rows at the medial (CM) side of the epithelium. Type-F cells were located at the sides of the epithelium in the medial most half. In the center area of the epithelium, type-E cells were found. Type-A cells were located at the saccular side of the epithelium. The hair-cell polarization was almost uniformly from

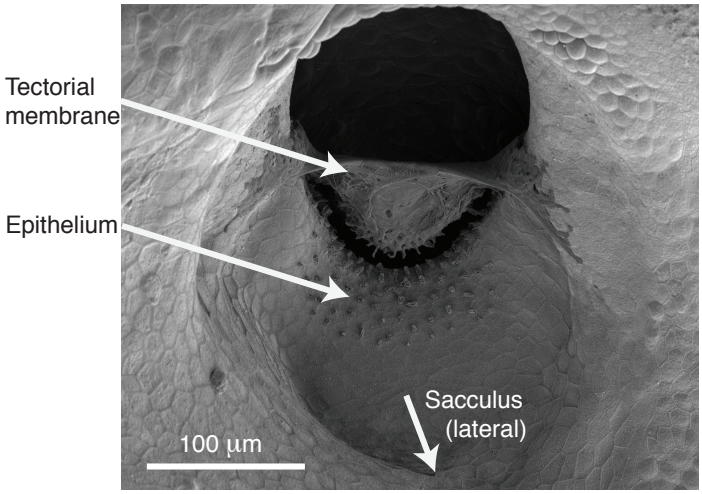

Figure 3.3: SEM image of the BP, viewed from the saccular side. The TM, with its extensive coupling to the lumen boundary is visible, as well as the hair bundles in the epithelium. The TM is reduced in size and detached from the epithelium due to the preparation process. The CM is located behind the epithelium and invisible in this view.

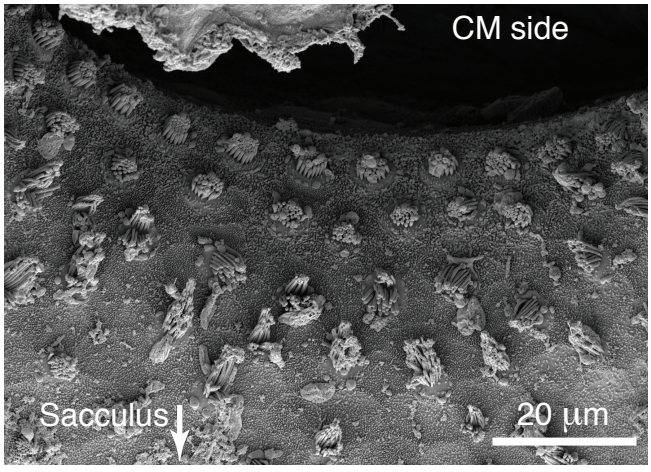

Figure 3.4: SEM image of part of the sensory epithelium in the BP. A regular organization of the hair cells is visible in the two rows at the CM side of the epithelium.

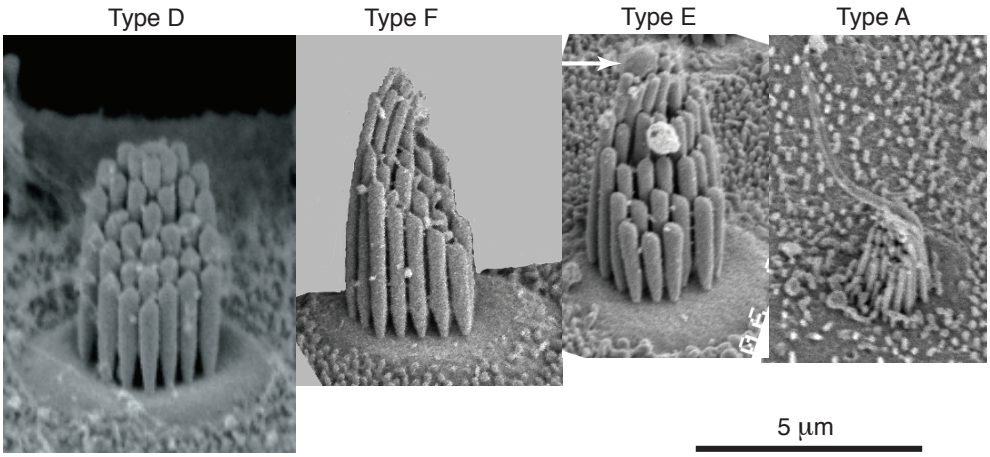

Figure 3.5: Four different types of hair cells identified in the BP. The individual panels are zoomed-in parts taken from different SEM images of the epithelium. The classification is according to Lewis and Li (1975). In type-D cells, the slope of the hair bundle is relatively low, and the maximum villus length is $\sim$ 3-4 μm; the kinocilium is bulbed. Type-F bundles have a steeper slope, a maximum height of $\sim$ 5-8 μm, and an unbulbed kinocilium. Type-E cells are similar to type-F cells except for a bulbed kinocilium (indicated by white arrow). Type-A cells have relatively short stereovilli and a tall unbulbed kinocilium ($\sim$ 5-8 μm).

the saccular side to the CM side of the epithelium. As an illustration, we superposed the distribution of the various types of hair cells across the epithelium and the hair-cell polarizations onto an SEM image of the BP in figure 3.6.

3.3.3 The tectorial membrane

The tectorial membrane had a semicircular shape. At a height of 100 to 150 μm (fig. 3.1) above the base of the epithelium (as displayed in the figures), a voluminous strand of tectorial material spanned the width of the lumen on the CM side of the epithelium. As is visible in figure 3.3, the connections of this strand to both sides of the lumen are bulky and project towards the sacculus along a large part of the length of the lumen. The width at the top of the TM was approximately 250 μm (determined from LM images).

From the strand of tectorial material, the TM extended towards the epithelium. In the images of non-fixated preparations, the TM could be observed to extend all the way onto the epithelium (fig. 3.7). From SEM images, additional information about the relationship between the TM and the epithelium could be obtained, although the direct connection between the epithelium and the TM had been lost due to the dehydration during post-fixation. In the images, the TM exhibited two to three rows of holes along its width on the side facing the epithelium (fig 3.8a). On the epithelium surface, remnants of connective tissue were visible on and around the hair bundles of the first two to three rows on the medial side of the epithelium (CM side, fig. 3.8b). Presumably, these rows of hair bundles extended into the holes in the TM, while the membrane itself connected to the microvilli surrounding the hair bundles.

The thickness of the TM (along the length of the lumen) was determined from images of

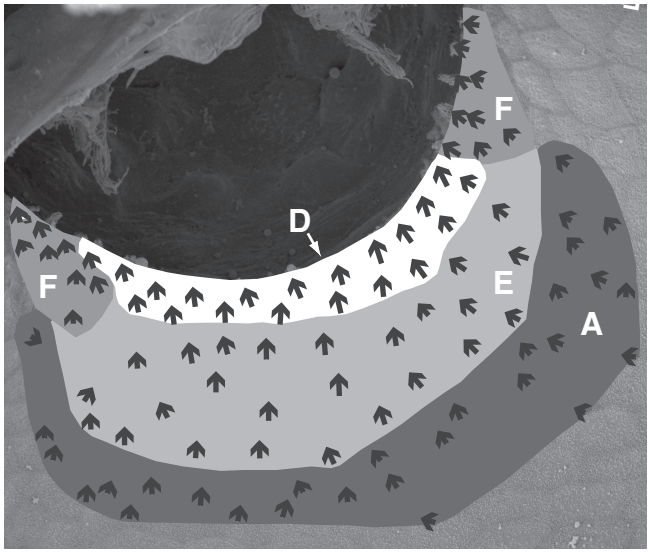

Figure 3.6: Distribution of the various types of hair cells across the epithelium and hair-cell polarization, superposed on a SEM image of the BP. Each arrow indicates an individual hair cell. Type-D cells (white) are located in the first rows on the CM side of the epithelium. Type-F cells (semi-dark gray) are found to the sides of the first rows of the epithelium. Type-E cells (light gray) are located in the center of the epithelium. Type-A cells (dark gray) occupy the sacullar-side of the epithelium. The type indications are given in white in the figure. The arrows indicate the hair-cell polarizations, based on the hair-bundle shape.

non-fixated preparations. In four preparations we chose six regions on the semicircular TM (fig. 3.9): in the middle near the top (region 1), on both sides near the lumen boundary at approximately half the height (regions 2 and 3), two near the epithelium in the lower part of the TM (regions 4 and 5), and one in the center of the TM (region 6). By moving the focal plane of the microscope along the lumen's length, the sharpness of the structure of the TM in each region indicated whether the focal plane was within or outside of the TM, and produced a measure of its thickness. On average the TM was 33 μm thick (range 18-50 μm). In the center (region 6), and near the top it was thicker, 38 μm (range 34-44 μm) and 46 μm (range 42-50 μm), respectively. At the epithelium, the TM was thinnest, on average 23 μm (range 18-36 μm). From the connective-tissue remnants on the epithelium in SEM images (e.g. fig. 3.8b), we determined the TM to epithelium connection to be about 20 μm, as well. Thus, the TM tapered towards its connection to the epithelium.

3.3.4 Overall image

In order to bring together the results from sections 3.3.1 through 3.3.3, an overview of the BP was created in blue-print style (fig. 3.10). The drawing displays the average BP of the northern leopard frog to the best of our current knowledge. In the overview, we combined the measurements discussed above.

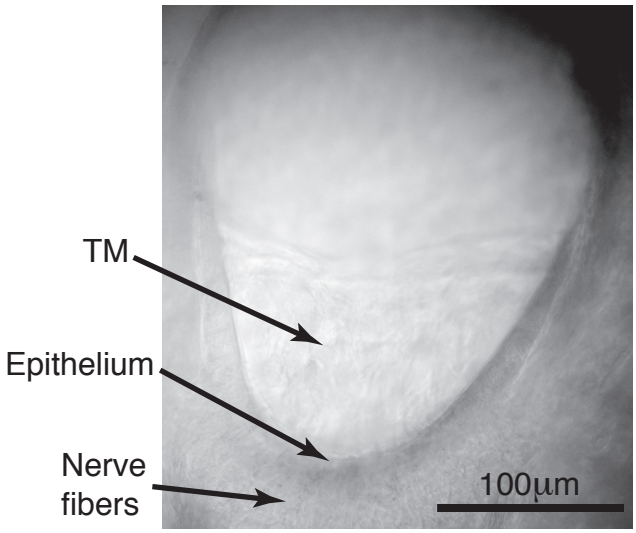

Figure 3.7: LM image of a non-fixated preparation. The TM, the epithelium and the connecting nerve-fibers are indicated. The TM extends to the epithelium. Adapted from Schoffelen et al.(2009b), figure 2; chapter 4

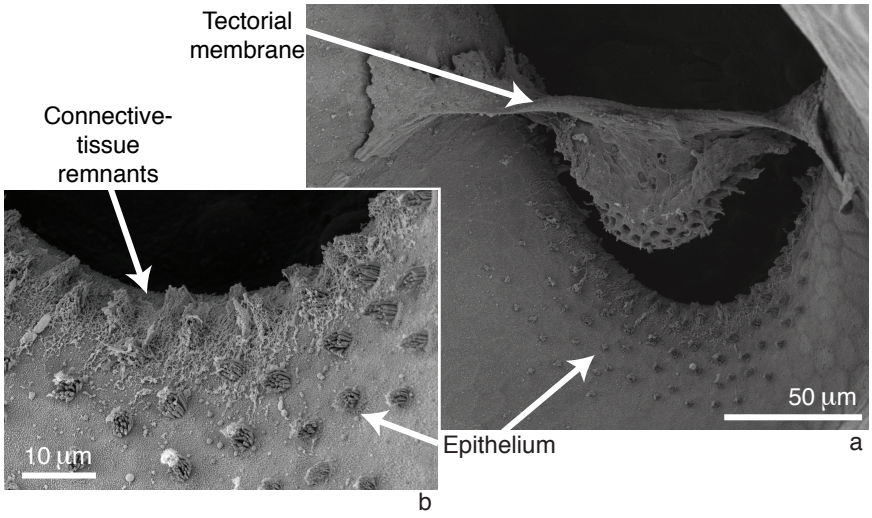

Figure 3.8: SEM image of the BP. *a:* Overview of the lumen, the TM and the epithelium. The holes are visible on the bottom part of the TM. The holes in the TM mirror the regular organization of the first two to three rows of hair cells (fig. 3.4) *b:* Zoomed image of the epithelium at the CM side of the lumen. The remnants of the connective tissue are visible on and between the upper rows of hair bundles in the image.

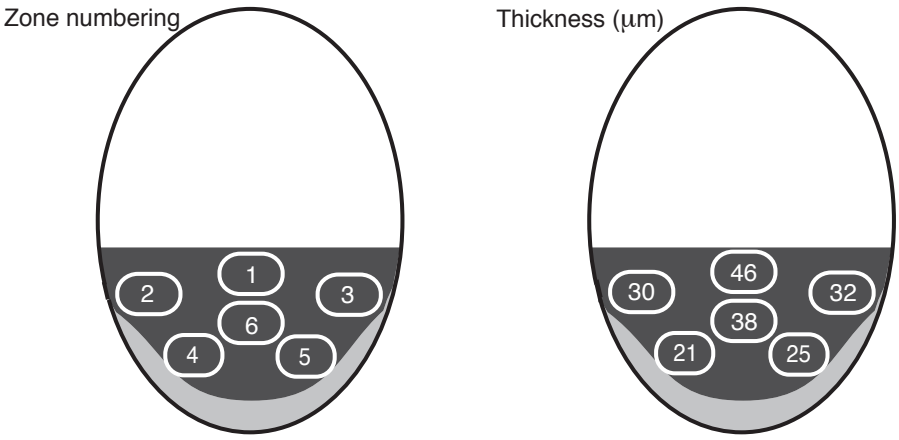

Figure 3.9: Thickness of the TM. The left panel shows the numbering of the zones used for determining the thickness of the TM in four preparations. In the right panel, the average thickness of the TM per zone is given in μm.

3.4 Discussion

For our images we used the ears of adult leopard frogs, aged from several months to about a year and a half. The data presented in this paper were collected over a period of approximately one year. We did not investigate the influence of age or sex of the animal on our results. Overall, our data from the northern leopard frog is in correspondence with earlier reports on related species. The general shape of the organ and its lumen corresponded to those reported in other derived anuran basilar papillae (e.g. *R. catesbeiana*, Van Bergeijk 1957, Frishkopf and Flock 1974, Lewis 1977; Xenopus laevis, Bergeijk and Witschi 1957; overview in Wever 1985).

The dimensions of the BP lumen were larger than those reported for the bullfrog. There, the width of the lumen is approximately 150 μm (Bergeijk and Witschi 1957), while its height is reported to be about 200 μm by Bergeijk and Witschi (1957). However, it appears to be somewhat larger in some specimens (Frishkopf and Flock 1974, fig. 2). The width (270 μm) and height (350-400 μm) we determined were considerably higher. This difference may be due to the fact that the bullfrog estimations were done on young adult specimens (Bergeijk and Witschi 1957; Frishkopf and Flock 1974), or even tadpoles (Bergeijk and Witschi 1957), while our measurements resulted from full-sized adult specimens. Another explanation may lie in different definitions of the width and height of the lumen. These are not detailed by Bergeijk and Witschi.

The average number of sensory hair cells in the BP was 76, based on SEM images. The variation between individual preparations was considerable (63 to 95), and we even counted as many as 115 hair cells, in one LM preparation. Coinciding with the larger dimensions of the lumen, we found more hair cells than were found in the bullfrog ($\sim$ 60, Bergeijk and Witschi 1957; Geisler et al. 1964), although Wever (1985) reports hair-cell counts of 95 and 99 in a bullfrog. Our average was within the expected range for the family of *Ranidae* (47-115 across various species, Wever 1985).

We identified four types of hair cells in the basilar papilla based on the shape of their

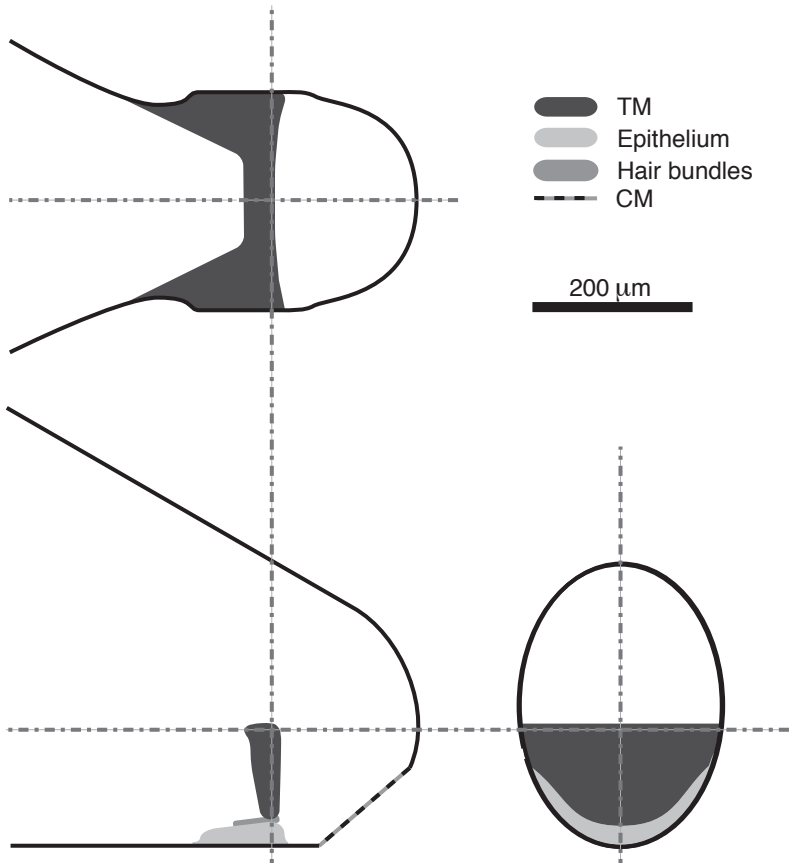

Figure 3.10: Cross sections of the BP, viewed from three directions. Sizes are based on the measurements described in the Results section. Some estimations and inferences have been used in the drawing, especially for the shape of the TM and the diameter of the CM.

ciliary tufts. This is one more type than Lewis and Li (1975) report for the BP of the bullfrog. While we identified type-A, type-D, type-E and type-F cells in the BP of the northern leopard frog, Lewis and Li do not report finding type-E cells in the BP of the bullfrog. The four types of cells were distributed systematically over the epithelium (fig. 3.6). The hair-cell polarization was uniformly from the saccular to the CM side of the epithelium. This polarization coincided with that reported in the bullfrog (Frishkopf and Flock 1974), and with polarization maps of other derived basilar papillae in anurans (Lewis et al. 1985; Lewis and Narins 1999).

Due to its tendency to shrink during fixation and dehydration procedures used in preparation for LM and SEM (see above, Frishkopf and Flock 1974), the determination of the TM's size and shape had more uncertainty than the other measurements reported here. From the SEM images and images of non-fixated preparations, the general shape of the TM was found to correspond to that reported in the bullfrog (Bergeijk and Witschi; Van Bergeijk; Geisler et al. 1964). It was semi-circular in shape, about 100 to 150 μm heigh, and approximately 250 μm wide at its maximum. Its thickness was on average 33 μm, at the connection to the epithelium it was about 20 μm. Even at the connection to the epithelium the thickness was

considerably higher than the reported measurement for *R. utricularia sphenocephala* (12 μm, Wever 1985).

The TM appeared to connect to the hair cells only at the most medial (CM) side of the epithelium. The pattern of the holes in the TM facing the epithelium appeared to mirror the dense and regular setting of the hair cells in the first rows on that side of the epithelium. Therefore, we infer that most likely the hair-bundles of the type-D cells (in the medial two to three rows of the epithelium) protrude into the holes in the TM. It is unclear whether the type-F cells protrude into the holes in the TM. We did not find any indication that the remaining hair cells (types E and A) were directly associated with the overlying TM. We therefore presume that these cells are in fact free-standing, in agreement with Lewis (1977) and Lewis and Narins (1999) and in disagreement with Wever (1985).

The dense packing and regular pattern of the hair cells connecting to the TM form an interesting correspondence between the frog's basilar papilla and other vertebrate hearing organs (e.g. the outer hair cells of the mammalian cochlea; Yost 2000). In mammals, the regular pattern of the outer hair cells has been suggested to play a key role in the tuning of the cochlea through the associated micro-fluid dynamics (Bell and Maddess 2009). At this point we can not exclude, nor support, a similar significance of the hair-cell pattern in the frog BP.

Overall, our detailed exploration of the northern leopard frog's basilar papilla did not produce any remarkable new results. As mentioned above, our findings were in line with descriptions of comparable species. The data presented in this paper must therefore be viewed as an incremental addition to the knowledge of the anuran basilar papilla. It is, to our knowledge, the most extensive description of the organ in this particular species.

Acknowledgements

We thank J. Kuipers, F. Dijk and dr. J.J.L. van der Want (Cell Biology-Medical Electron Microscopy, University Medical Center Groningen) for their assistance and support in conducting the work presented in this paper.

This study was supported by the Heinsius Houbolt Foundation and the Netherlands Organisation for Scientific Research, and is part of our department's research program: Communication through Hearing and Speech.